



The Construction of Generalized Magnetic Coordinates

Michinari Kurata

*Dept. of Energy Engineering and Science,
Graduate School of Engineering, Nagoya University*

and

Jiro Todoroki

National Institute for Fusion Science

Abstract

Generalized Magnetic Coordinates (GMC) are curvilinear coordinates (ξ, η, ζ) in which the magnetic field is expressed in the form

$$\mathbf{B} = \nabla\Psi(\xi, \eta, \zeta) \times \nabla\zeta + H^s(\xi, \eta) \nabla\xi \times \nabla\eta.$$

The GMC construction algorithm is applied to the simple periodic model magnetic field. The coordinates are expanded in the Fourier series in three dimensions. It is obtained after about 10~35 times iterations. The coordinates are well constructed by the comparatively small number of Fourier modes.

Keywords:

generalized magnetic coordinates, GMC, magnetic flux coordinates, magnetic surface, magnetic islands, ABC magnetic field, Fourier series, B-spline function

§ 1. Introduction

Magnetic flux coordinates[1,2] are widely used in the study of the MHD equilibrium and stability in the toroidal plasma when the nested magnetic surfaces exist. Unfortunately, the nested magnetic surfaces exist only in the limited region of torus; and even inside the outermost magnetic surface there might exist complicated magnetic islands structure. In such cases, the use of the conventional magnetic flux coordinates is not expected.

The Generalized Magnetic Coordinates (GMC)[3] are the new one to supplement the magnetic coordinates system adequate to treat the general magnetic configurations. The GMC can be constructed in the region without nested magnetic surface and the region of chaotic or ergodic magnetic lines of force. So the GMC can treat the magnetic field involving magnetic islands and outside the outermost magnetic surface.

In the GMC (ξ, η, ζ) the magnetic field is expressed in the form

$$\mathbf{B} = \nabla\Psi(\xi, \eta, \zeta) \times \nabla\zeta + H^s(\xi, \eta) \nabla\xi \times \nabla\eta, \quad (1)$$

here $H^\zeta \equiv \sqrt{g}B^\zeta$ does not depend on ζ , where \sqrt{g} is Jacobian. The function Ψ is the covariant ζ component of vector potential. When the good magnetic surface exists, Ψ becomes independent of ζ and $\Psi(\xi,\eta)=\text{Const.}$ is the magnetic surface. The ζ -dependent part of Ψ corresponds to the destruction of the magnetic surface. The GMC are to be constructed so that the ζ component of vector potential becomes dependent of ζ as little as possible.

In order to check the GMC construction algorithm, the general numerical method to construct a GMC is applied to the simple periodic model magnetic field[4,5]. In this paper the GMC are applied to the model magnetic field involving clearly magnetic islands.

§ 2. Construction of GMC

The algorithm to construct GMC is the new one to construct magnetic surfaces without tracing magnetic lines of force. It is based on the transformation rule of the vector potential accompanied with the change of coordinates[3].

We shall consider a curvilinear coordinate system (ξ, η, ζ) , ζ being the angle variable corresponding to the toroidal direction. We introduce a time-like parameter τ and consider the continuous path from an initial state of coordinates to the GMC. Then coordinates are expressed as follows,

$$\mathbf{r}=\mathbf{r}(\xi,\eta,\zeta;\tau). \quad (2)$$

The coordinates approach to GMC when $\tau \rightarrow \infty$. The parameter τ corresponds to the iteration time in numerical calculation by computer.

The magnetic induction densities $\sqrt{g}\mathbf{B}=(H^\xi, H^\eta, H^\zeta)$ can be expressed in terms of the vector potential $\mathbf{A}=(A_\xi, A_\eta, A_\zeta)$ as

$$H^\xi = \frac{\partial A_\zeta}{\partial \eta} - \frac{\partial A_\eta}{\partial \zeta}, \quad H^\eta = \frac{\partial A_\xi}{\partial \zeta} - \frac{\partial A_\zeta}{\partial \xi}, \quad H^\zeta = \frac{\partial A_\eta}{\partial \xi} - \frac{\partial A_\xi}{\partial \eta}. \quad (3)$$

If we introduce the notations

$$\bar{A} \equiv \oint A d\zeta / \oint d\zeta, \quad \tilde{A} \equiv A - \bar{A}, \quad (4)$$

the principles to construct The GMC can be expressed by the following conditions;

- 1) H^ζ does not depend on ζ ,
- 2) \tilde{A}_ζ is minimized,

which are represented as

$$\oint |\tilde{H}^\zeta|^2 d\zeta = 0, \quad \delta \oint |\tilde{A}_\zeta|^2 d\zeta = 0. \quad (5)$$

§ 3. Modeling and Results

We employ the ABC(Arnol'd-Beltrami Childress) magnetic field in the Cartesian coordinates added constant magnetic field in the direction of z as the model magnetic field,

$$\begin{aligned}
B_x &= b \cos(2\pi y) + c \sin(2\pi z), \\
B_y &= c \cos(2\pi z) + a \sin(2\pi x), \\
B_z &= a \cos(2\pi x) + b \sin(2\pi y) + B_0
\end{aligned} \tag{6}$$

with $(a=0.2, b=0.1, c=0.6)$. This magnetic field is periodic in the directions of (x, y, z) . The constant magnetic field B_0 is added so that $B_z > 0$.

The (x, y, z) coordinates are expanded into Fourier series in terms of the GMC (ξ, η, ζ) ,

$$\begin{aligned}
x &= \xi + \sum_{l=-L}^L \sum_{m=-L}^L \sum_{n=1}^L X_{l,m,n} \exp(2\pi i[l\xi + m\eta + n\zeta]), \\
y &= \eta + \sum_{l=-L}^L \sum_{m=-L}^L \sum_{n=1}^L Y_{l,m,n} \exp(2\pi i[l\xi + m\eta + n\zeta]), \\
z &= \zeta.
\end{aligned} \tag{7}$$

The space is divided into 20~40 meshes of (ξ, η, ζ) . The scalar function v is also expanded by Fourier series. The GMC are obtained after about 10~35 times iterations so far.

In the previous paper[5], we reported two magnetic field cases of $B_0=0.5, 1.0$ without involving clearly magnetic islands using the number of Fourier mode from $L=1$ to $L=7$. Fig.1 shows the Poincaré maps of magnetic surfaces of $B_0=1.0$ on the $\zeta=0$ plane in the GMC. Fig.2 shows the shape and contour of $\bar{A}_\zeta(\xi, \eta)$. When the nested magnetic surfaces exist, they are equal to $\bar{A}_\zeta = \text{Const.}$.

Next, the constant B_0 is lowered to $B_0=0.45$, so that the magnetic field involves clearly magnetic islands. The variation of the magnetic field in the ζ direction is larger than the case of $B_0 = 0.5$. Fig.3 shows the GMC mesh of $\xi, \eta = \text{Const.}$ at equal intervals constructed in the number of Fourier mode $L=9$ on the $z=0, 0.25, 0.5, 0.75$ planes in the Cartesian coordinates. The Poincaré maps of magnetic surfaces of $B_0=0.45$ is also overlapped in Fig.3. The only central toroidal field of interest is drawn in the Poincaré map and the outside of it is omitted to draw. Fig.4 shows the Poincaré maps of magnetic surfaces on the $\zeta=0, 0.25, 0.5, 0.75$ planes in the GMC. The magnetic islands of poloidal mode number $M=5, 7$ and 9 are clearly shown. The magnetic islands rotate as ζ changes. Fig.5 shows the shape and contour of averaged magnetic surface $\bar{A}_\zeta(\xi, \eta)$. The averaged magnetic surface is $\bar{A}_\zeta = \text{Const.}$ when the breaking of nested magnetic surfaces exist. Fig.6 shows the Poincaré map on the $\zeta=0.75$ plane overlapped to Fig.5. The magnetic islands of $M=5$ rotate along the averaged magnetic surface; and the width of magnetic islands of $M=5, 9$ could be measured by the averaged magnetic surface.

In order to evaluate the magnitude of the ζ dependent part of H^ζ , we calculate the integral,

$$I_\zeta = \int_0^1 \int_0^1 \int_0^1 |\tilde{H}^\zeta|^2 d\xi d\eta d\zeta. \tag{8}$$

The integral I_ζ is plotted against the number of Fourier mode L in Fig.7. It decreases exponentially as L increases. Since the GMC are constructed so that \tilde{H}^ζ becomes zero, I_ζ must converge to zero. So the error of I_ζ is caused by the finite truncation error for the most part.

In order to estimate the influence from the breaking of magnetic surfaces, we evaluate the magnitude of the ζ

dependent part of H^ξ and H^η by the integral,

$$I_\xi = \int_0^1 \int_0^1 \int_0^1 |\tilde{H}^\xi|^2 d\xi d\eta d\zeta, \quad I_\eta = \int_0^1 \int_0^1 \int_0^1 |\tilde{H}^\eta|^2 d\xi d\eta d\zeta \quad (9)$$

The integral I_ξ and I_η are plotted in Fig.7. Since \bar{A}_ζ is minimized in the GMC, \tilde{H}^ξ and \tilde{H}^η are also minimized. Since \tilde{H}^ξ and \tilde{H}^η naturally contain the contribution from magnetic islands where the nested magnetic surface does not exist, only its contribution should be contained in I_ξ and I_η if the GMC are precisely made up. Since both I_ξ and I_η are not saturated and they are not very different from I_ζ , they are mostly reflected by the smallness of number of Fourier mode more than the breaking of magnetic surfaces.

In order to estimate \tilde{A}_ζ that relates with the breaking of magnetic surfaces, we calculate the integral,

$$E_{\xi\eta}(\xi, \eta) = \int_0^1 (|\tilde{H}^\xi|^2 + |\tilde{H}^\eta|^2) d\zeta. \quad (10)$$

The shape and contour of $E_{\xi\eta}$ are shown in Fig.8. The shape of $E_{\xi\eta}$ seems like a crater of volcano. The shapes are roughly unchanged for the number of Fourier mode from L=1 to L=9, but the shapes become a deeper crater as L increases. Although the magnetic islands of poloidal mode number M=5 locate in the middle of the magnetic axis and the outermost magnetic surface, $E_{\xi\eta}$ is not especially large there. The largest region of $E_{\xi\eta}$ is annular and located around the outside of the outermost magnetic surface. The region of nested magnetic surfaces around the magnetic axis corresponds to the region of smaller $E_{\xi\eta}$. The similar result for $E_{\xi\eta}$ is obtained for the magnetic field of $B_0=0.5$.

At last, in order to examine the distribution of \tilde{H}^ζ , we calculate the integral

$$E_\zeta(\xi, \eta) = \int_0^1 |\tilde{H}^\zeta|^2 d\zeta. \quad (11)$$

The shape and contour of E_ζ are shown in Fig.9. Since the shape of E_ζ is similar to $E_{\xi\eta}$, the region of the outside of outermost magnetic surface influences on the convergence of E_ζ alike. Although E_ζ must converge to zero like I_ζ , the shape of E_ζ approaches to that of $E_{\xi\eta}$ if L becomes large to L=9. The meaning of this is not clear at the present.

§ 4. Summary

It is shown that the averaged magnetic surface $\bar{A}_\zeta = \text{Const.}$ is equal to the magnetic surface when the nested magnetic surfaces exist. The GMC can be constructed for the magnetic field involving clearly magnetic islands by the general algorithm to construct GMC. In this model field H^ξ, H^η and H^ζ decreases exponentially as the number of Fourier mode increases. The distribution of \tilde{A}_ζ that relates with the breaking of magnetic surfaces is estimated. The largest region of \tilde{A}_ζ is located around the outside of the outermost magnetic surface. The relationship between \tilde{A}_ζ and the region where magnetic surface does not exist should be examined in further detail.

In the general magnetic configuration of interest the periodic condition in three dimension cannot be used. In order to drop the periodic conditions of magnetic field in ξ and η directions, the B-spline function should be used as the basis of expansion. The B-spline function that has local support is adequate to treat the general magnetic field involving further breaking of magnetic surfaces.

Reference

- [1] S.Hamada: Nucl. Fusion **2**, 23 (1962).
- [2] A.Boozer: Phys. of Fluids **24**, 1999 (1981).
- [3] J.Todoroki: 核融合研究における数値解析手法と最適化 (統計数理研究所共同研究レポート105), 1997, pp.1-10.
- [4] M.Kurata and J.Todoroki: J. Plasma Fusion Res. SERIES, Vol. 1 (1998) 491-494.
- [5] J.Todoroki and M.Kurata: 核融合研究における数値解析手法と最適化 (統計数理研究所共同研究レポート110), 1998, pp.1-10.

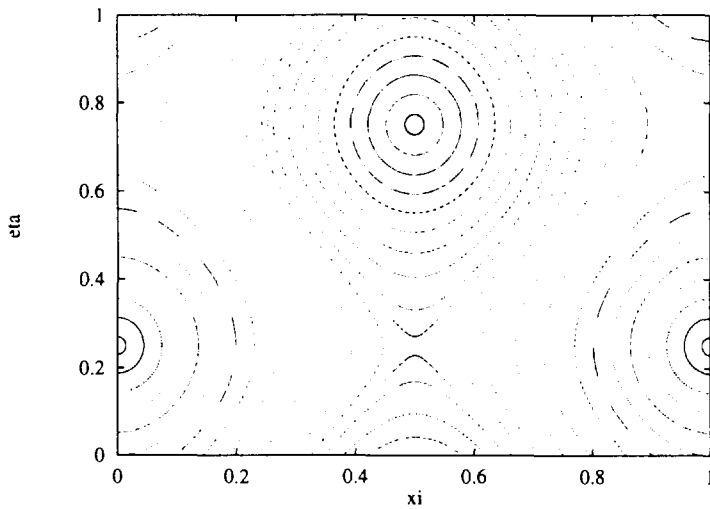


Fig.1. The Poincaré map at $\zeta=0$ in GMC (ξ, η, ζ)
($B_0=1.0, L=7$).

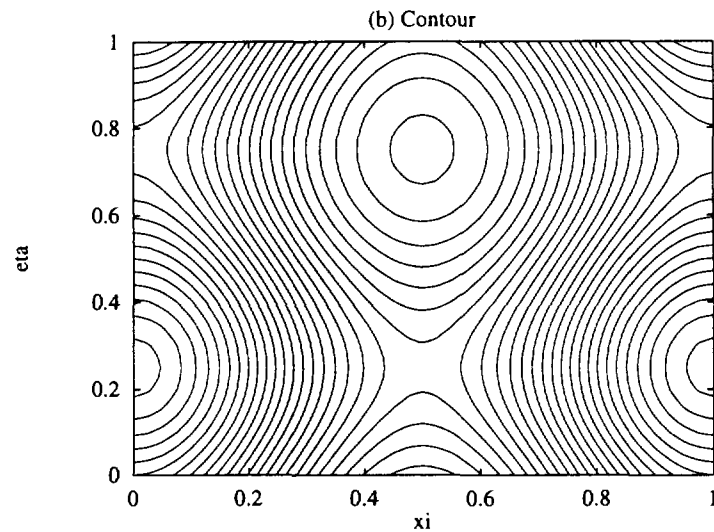
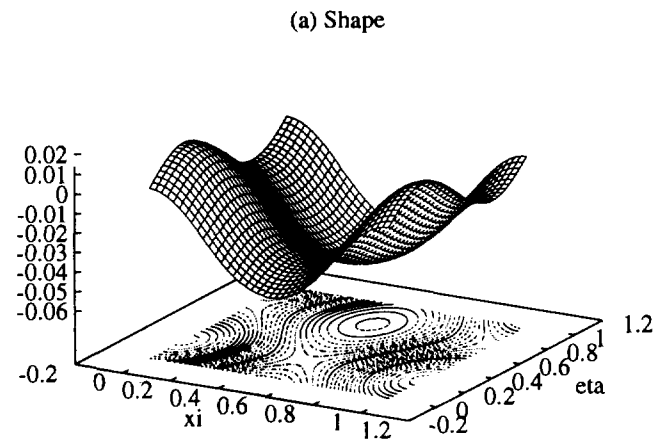


Fig.2. The shape and contour of $\bar{A}_\zeta(\xi, \eta)$ in GMC (ξ, η, ζ)
(a)Shape, (b)Contour ($B_0=1.0, L=7$).

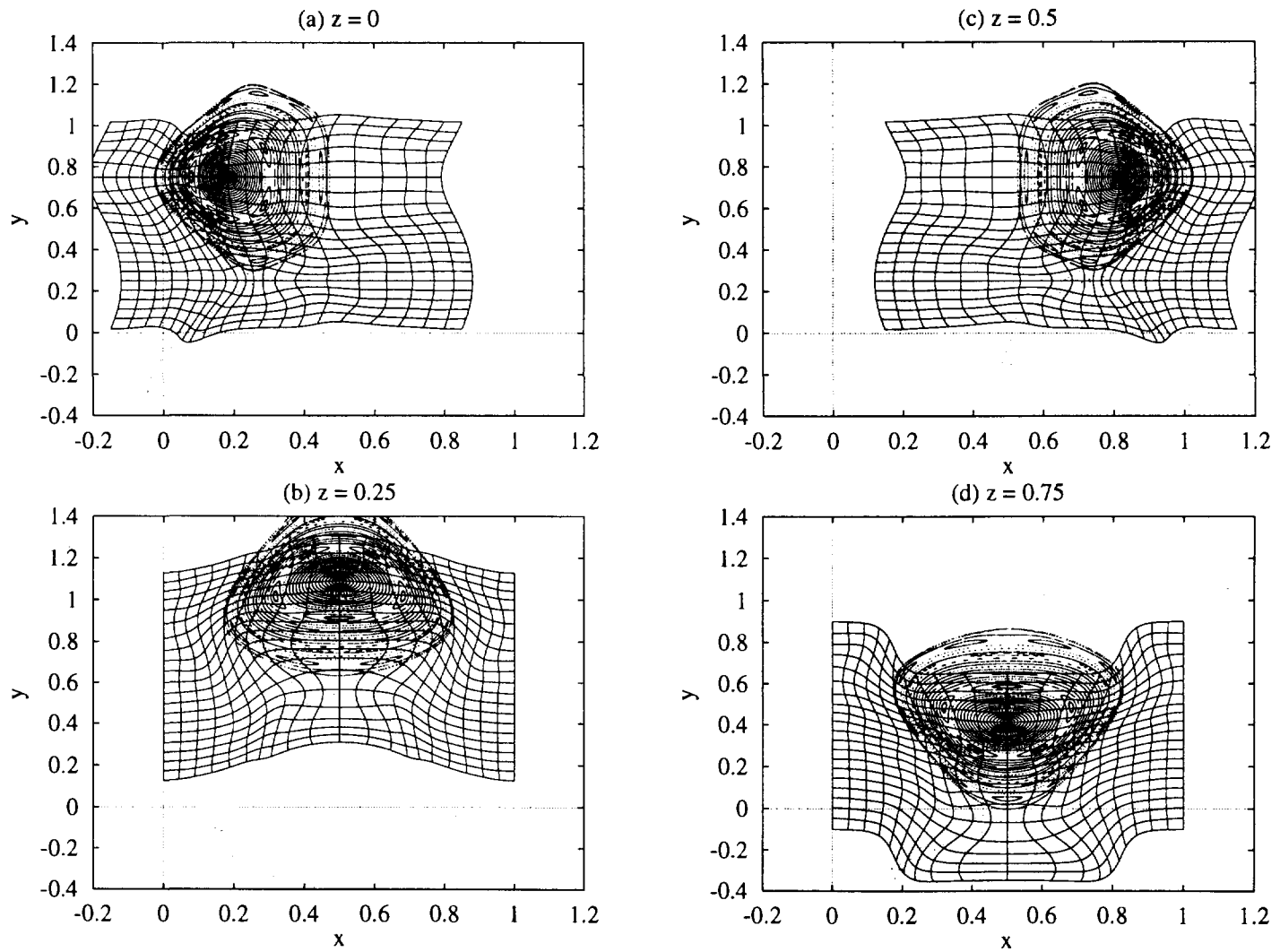


Fig.3. The GMC meshes and Poincaré map in (x,y,z) ($B_0=0.45, L=9$)

(a) $z=0$, (b) $z=0.25$, (c) $z=0.5$, (d) $z=0.75$.

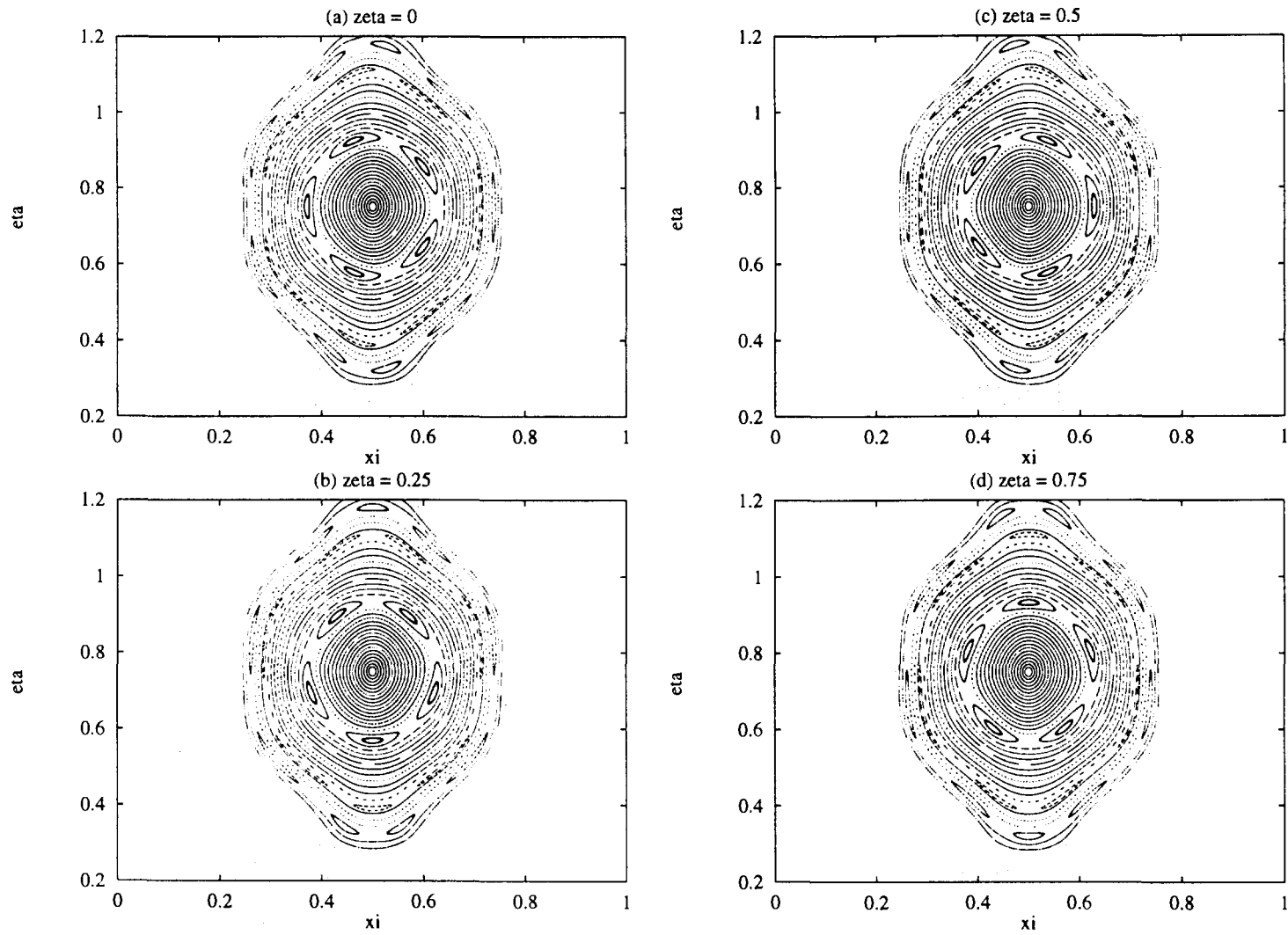


Fig.4. The Poincaré map in GMC (ξ, η, ζ) ($B_0=0.45, L=9$)
(a) $\zeta=0$, (b) $\zeta=0.25$, (c) $\zeta=0.5$, (d) $\zeta=0.75$.

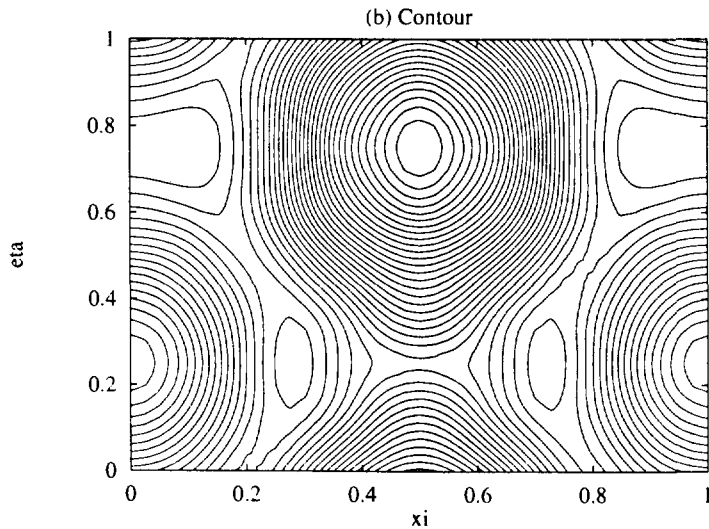
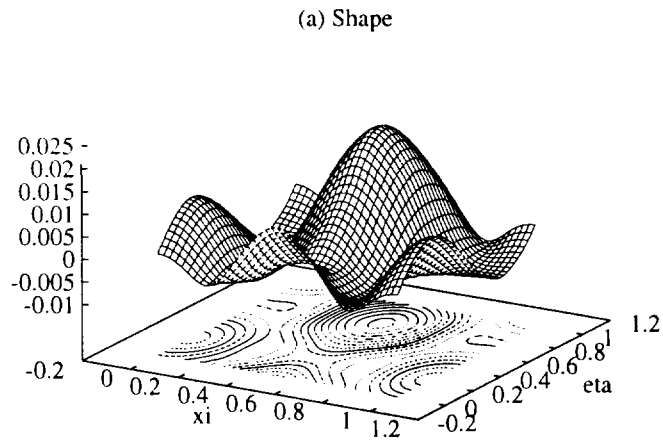


Fig.5. The shape and contour of $\bar{A}_z(\xi,\eta)$ in GMC (ξ,η,ζ) (a)Shape, (b)Contour ($B_0=0.45, L=9$).

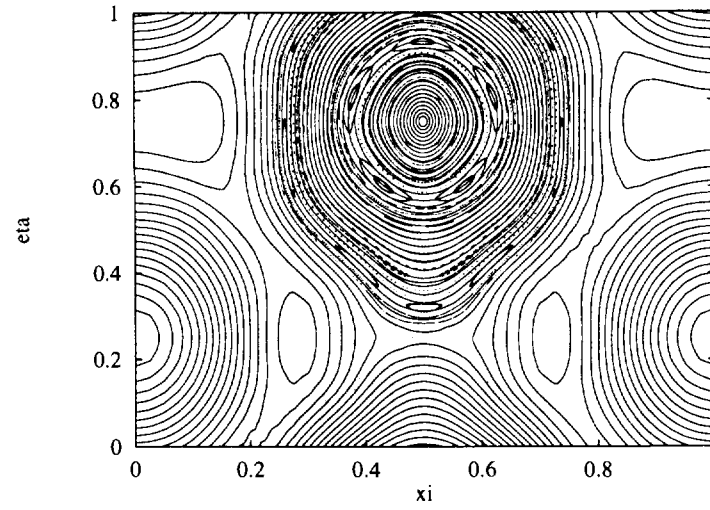


Fig.6. \bar{A}_z contour and Poincaré map at $z=0.75$ in GMC (ξ,η,ζ) ($B_0=0.45, L=9$).

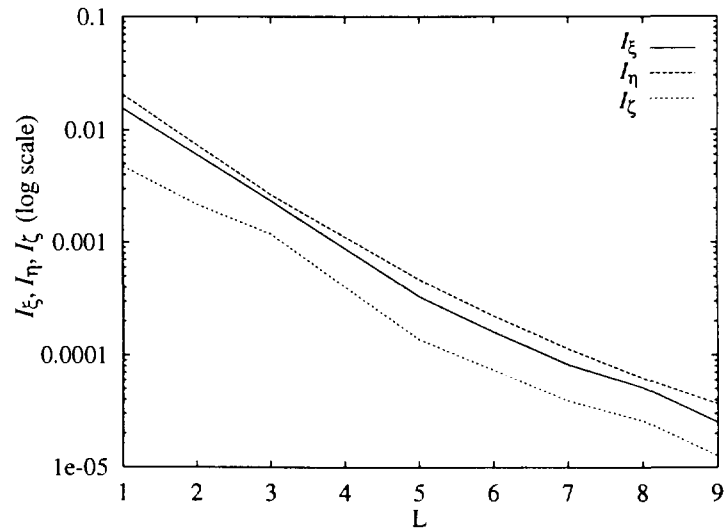


Fig.7. I_ξ, I_η and I_ζ vs. The number of Fourier mode L ($B_0=0.45$).

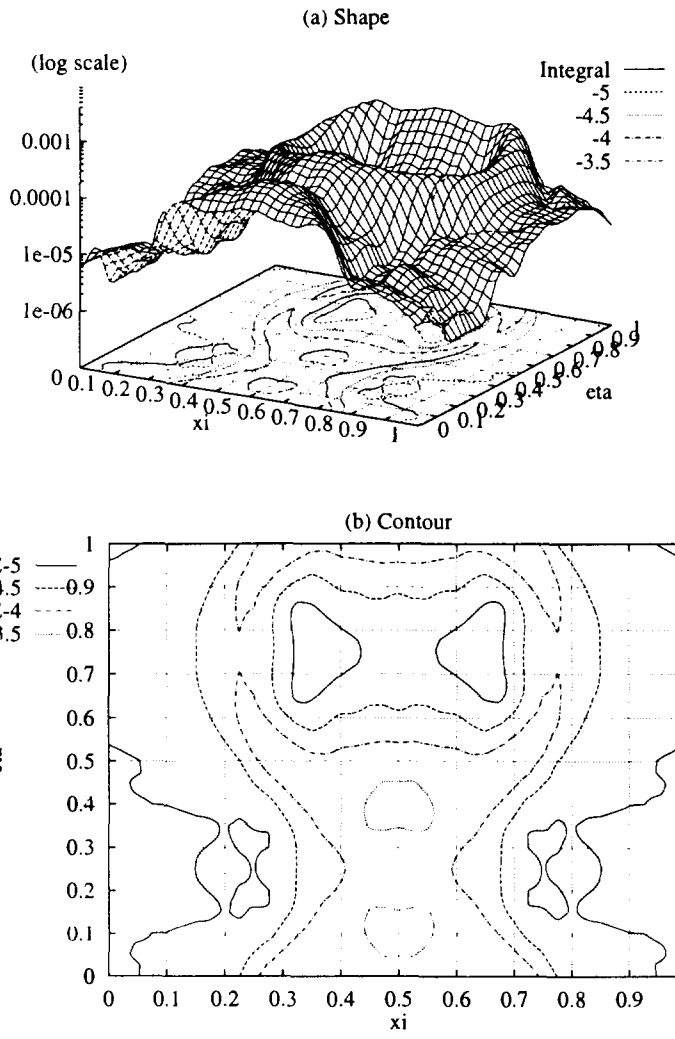


Fig.8. The shape and contour of $E_{\xi\eta}$ ($B_0=0.45, L=9$)
 (a)Shape, (b)Contour.

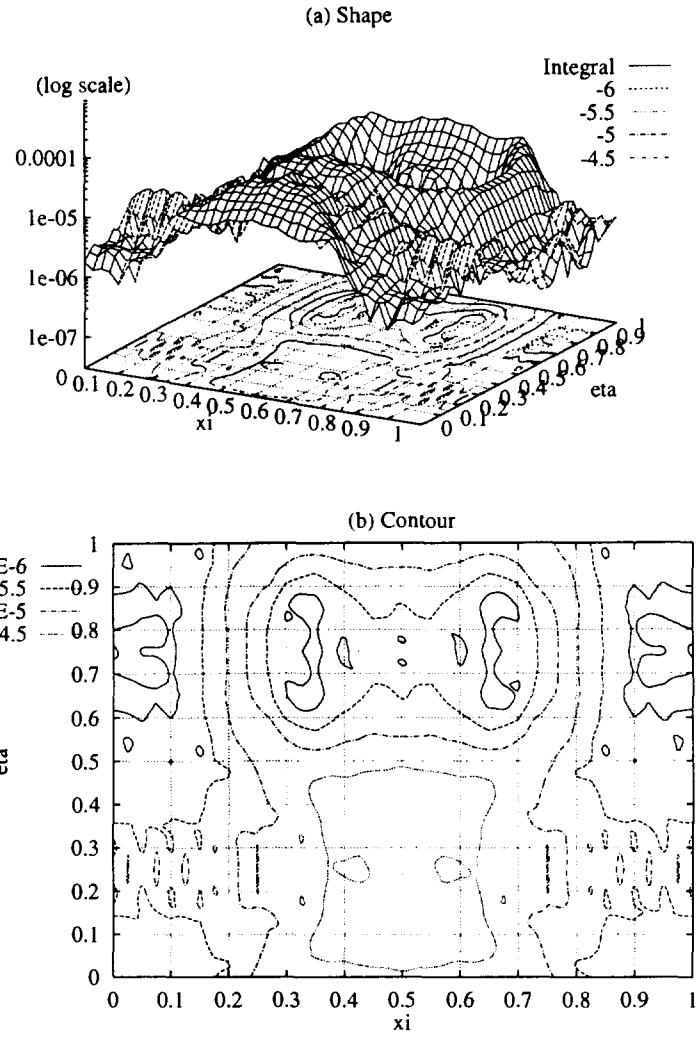


Fig.9. The shape and contour of E_{ζ} ($B_0=0.45, L=9$)
 (a)Shape, (b)Contour.